JEOL
Solutions for Innovation

Unlock the Potential of Multi-Resonance Experiments

Download the Guide

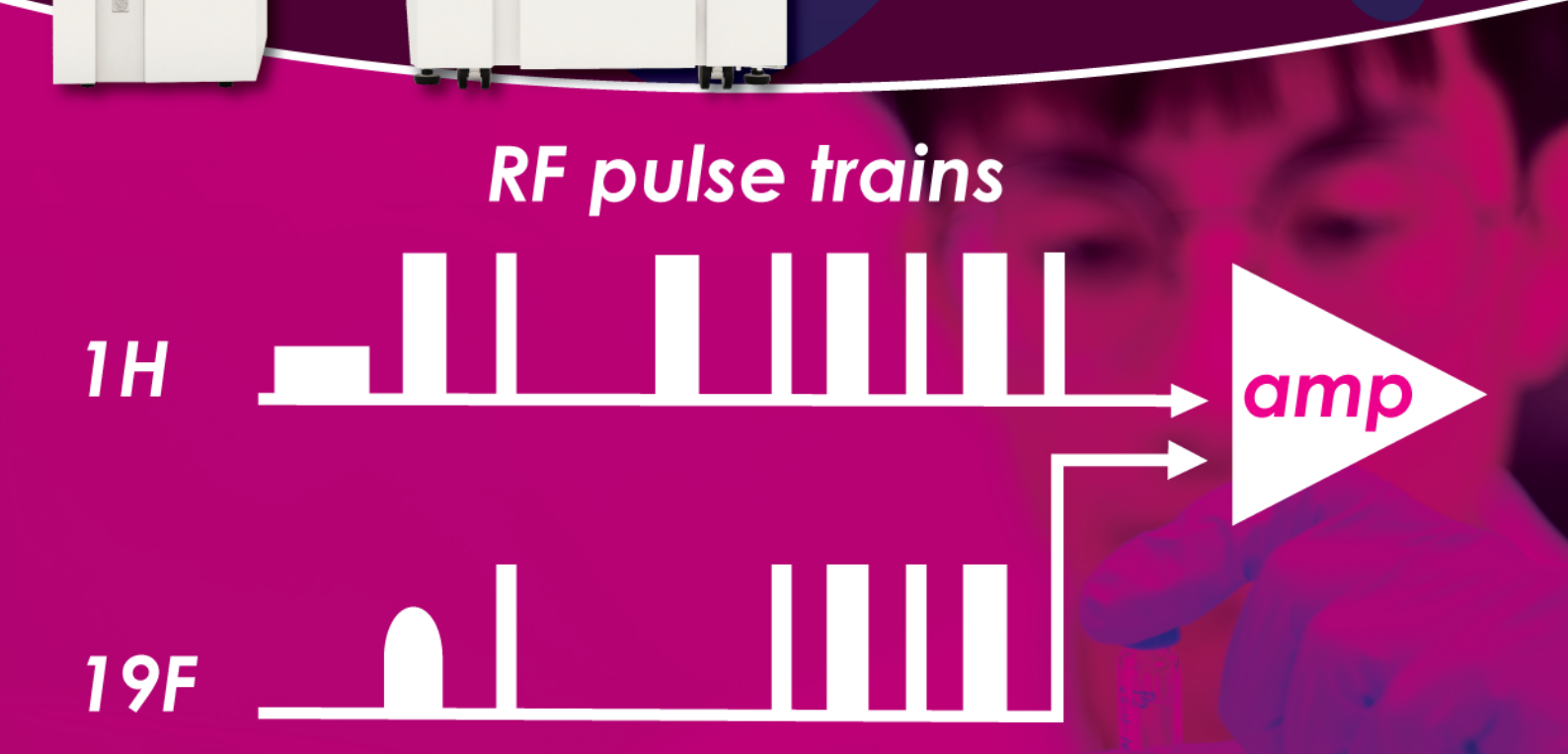

Received: 2 December 2022 | Revised: 12 September 2023 | Accepted: 18 September 2023

DOI: 10.1002/mrc.5402

RAPID COMMUNICATION

WILEY

Molecular precursors to produce para-hydrogen enhanced metabolites at any field

Anil P. Jagtap[1,2] | **Salvatore Mamone**[1,2] | **Stefan Glöggler**[1,2]

[1]NMR Signal Enhancement Group, Max Planck Institute for Multidisciplinary Sciences, Göttingen, Germany

[2]Center for Biostructural Imaging of Neurodegeneration, University Medicine Göttingen, Göttingen, Germany

Correspondence
Stefan Glöggler, NMR Signal Enhancement Group, Max Planck Institute for Multidisciplinary Sciences, Am Fassberg 11, Göttingen 37077, Germany.
Email: stefan.gloeggler@mpinat.mpg.de

Funding information
H2020 European Research Council, Grant/Award Number: 949180; Max Planck Society

Abstract

Enhancing magnetic resonance signal via hyperpolarization techniques enables the real-time detection of metabolic transformations even in vivo. The use of para-hydrogen to enhance ^{13}C-enriched metabolites has opened a rapid pathway for the production of hyperpolarized metabolites, which usually requires specialized equipment. Metabolite precursors that can be hyperpolarized and converted into metabolites at any given field would open up opportunities for many labs to make use of this technology because already existing hardware could be used. We report here on the complete synthesis and hyperpolarization of suitable precursor molecules of the side-arm hydrogenation approach. The better accessibility to such side-arms promises that the para-hydrogen approach can be implemented in every lab with existing two channel NMR spectrometers for ^{1}H and ^{13}C independent of the magnetic field.

KEYWORDS

hyperpolarization, metabolites, NMR, para-hydrogen, pyruvate

1 | INTRODUCTION

Nuclear magnetic resonance (NMR) is an insensitive phenomenon due to the small energy difference between nuclear spins that align parallel and antiparallel when brought into a magnetic field. The Boltzmann distribution of the nuclear spins leads to a population difference in which the lowest energy level is populated only by a few more parts per million than the other level. Despite this, NMR has become a valuable tool in analytical chemistry, metabolomics, structural biology, and in magnetic resonance imaging. The latter is being used daily in many clinics around the world.[1] To overcome sensitivity challenges, signal-enhancement or hyperpolarization approaches have been devised.[2–51] One important application of hyperpolarization is the real-time monitoring of metabolites that can be converted in vitro and in vivo.[3–7] It has been demonstrated in animals and patients that, for example, tumors are detectable by the conversion of hyperpolarized ^{13}C-pyruvate into lactate.[3–7,34] Until recently, this detection was only possible via a method named dissolution dynamic nuclear polarization for which a molecule of interest is cooled at cryogenic helium temperature and irradiated in the presence of radicals with microwaves for tens of minutes up to an hour.[2] After the polarization has built up in the solid, the sample is rapidly dissolved and brought to room temperature. The yielded polarized pyruvate in solution is afterwards injected for imaging. Para-hydrogen-based methods are other approaches to enhance the signals of metabolites.[7–51] Foremost, the para-hydrogen-induced polarization approach by means of sidearm hydrogenation (PHIP-SAH) was the first to demonstrate signal-enhanced metabolites.[22] For PHIP-SAH, an unsaturated

bond is attached to a ^{13}C-enriched metabolite of interest. This sidearm is then hydrogenated with para-hydrogen, and the obtained spin order is transferred to the ^{13}C spin to obtain enhanced signals. Cleavage of the side chain and work-up yields the hyperpolarized metabolite. Another para-hydrogen enhancement approach is based on Signal Amplification by Reversible Exchange whereby para-hydrogen is reacted with a metal complex and metabolite of interest yielding enhanced signals without the necessity of chemically altering the structure of the target compound.[39–50] Until recently, most studies have exclusively been performed in organic solvents, which made biological studies not feasible. However, one example has now been reported that pyruvate can be brought into an aqueous phase giving hope that future biological studies can follow.[50] PHIP-SAH to enhance pyruvate has so far been used for imaging and metabolic assessment of the heart and as recently shown by us to even provide sufficient signal for tumor imaging.[23,34] Since hyperpolarized metabolites are prepared in less than 1 min, para-hydrogen provides a scalable solution for future patient studies. We have furthermore shown that optimized strategies of PHIP-SAH precursors can lead to large degrees of pyruvate polarization at high concentrations. Depending on the molecular precursor design, hyperpolarized metabolites can be obtained with any pulsed NMR system and independent of the magnetic field.[30,32–34] In this article, we have investigated approaches for the synthesis of an isotopically labeled sidearm adapted for field-independent PHIP-SAH methodologies and report on its attachment to pyruvate and acetate as well as their polarization. Providing this sidearm starting from readily available compounds aims at providing further access to other labs of the PHIP-SAH technology and to implement it into existing hardware. Here, we demonstrate the PHIP-SAH method by polarizing pyruvate and acetate precursors at 21.5 mT.

2 | RESULTS AND DISCUSSION

Our field-independent approach for hyperpolarizing metabolites is shown in Figure 1a. The precursor includes two ^{13}C species, one located in an acetylene moiety and one in the metabolite of interest. After the addition of

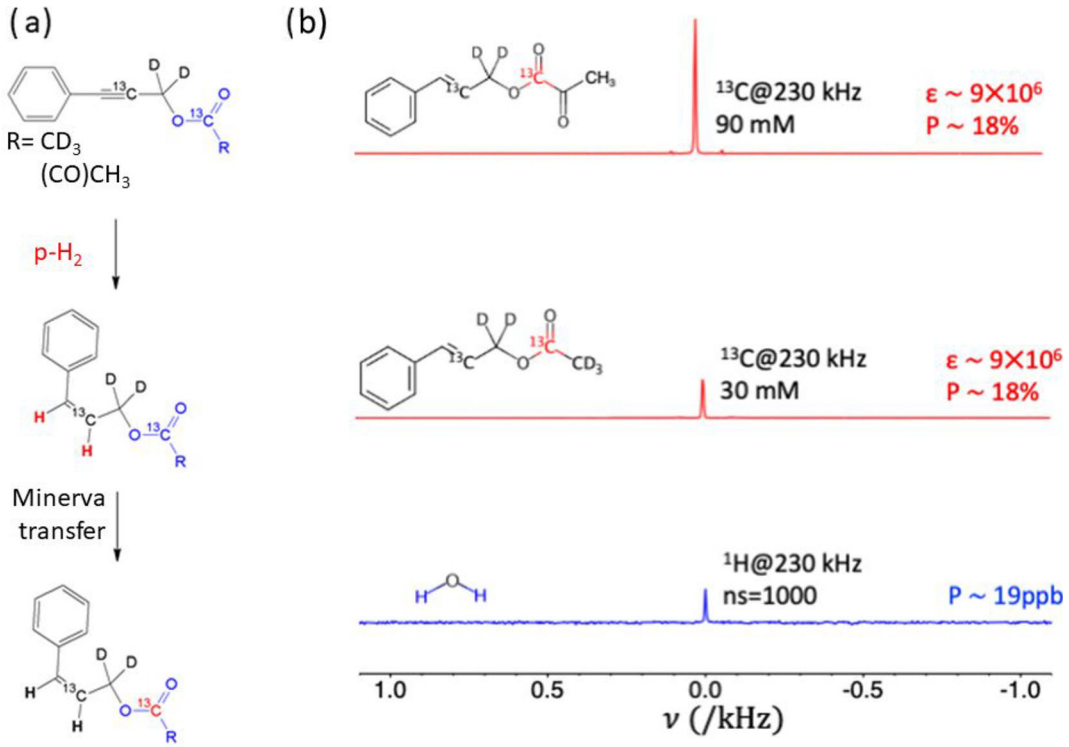

FIGURE 1 (a) Sidearm precursor and its hyperpolarization. Blue indicates the metabolite of interest and red para-hydrogen (p-H_2) and the hyperpolarized nuclear sites. (b) Polarization (P with enhancement factors ε) of the pyruvate and acetate precursors at ~21.5 mT. After hydrogenation and application of the pulse transfer sequence at ~21.5 mT, a large signal is observed on the ^{13}C channel frequency $\nu \sim 230$ kHz, corresponding to the ^{13}C label on the carbonyl site of the pyruvate (top) and acetate (bottom) moieties, respectively. The enhancement and polarization levels are calculated as discussed in the main text; see also Mamone et al.,[33] by reference to the ^{1}H signal of water recorded on the same coil at the same frequency (at a field of ~5.6 mT). The small signals on both sides of the main peak originate from a tiny residual magnetization left on the ^{13}C label on the sidearm, split into a doublet by the large one-bond J_{CH}-coupling ~160 Hz.

para-hydrogen, the J_{CH}-coupling of the proton directly bonded to the ^{13}C label in the sidearm is ~160 Hz, while the other (two-bond) J_{CH}-coupling is negligible. Such arrangement quenches the evolution under the flip-flop terms of the proton-proton scalar interaction, allowing for the application of field-independent polarization transfer methodologies. Moreover, the ^{13}C label on the sidearm allows relaying the magnetization to a target nucleus in species of interest further away from the hydrogenation site. Here, we applied the MINERVA protocol (Maximizing Insensitive Nuclei Enhancement Relayed Via para-hydrogen Amplification) to transfer the nascent spin order from para-hydrogen into heteronuclear magnetization.[32,33] In this study, we have coupled the sidearm to pyruvate and acetate and demonstrate that the ^{13}C label at the carbonyl position in the metabolite precursors can be polarized in high concentrations at 21.5 mT. The results of these experiments are depicted in Figure 1b. Previously, we have established that the cleavage of the labile ester bond between the cinnamyl sidearm and the molecule of interest followed by a fast purification method (developed in our group) releases the hyperpolarized metabolite in neat water solutions at physiological conditions.[32,33,51] These steps for full biocompatibility have been demonstrated for pyruvate recently.[32,33,51]

To synthesize the sidearm, readily available benzaldehyde **1** (CAS 100–52-7, Scheme 1) was reacted with a Grignard reagent, which was obtained by the reaction of ^{13}C-methyl iodide (CAS 207507-22-0) and magnesium (CAS 7439-95-4), to obtain the secondary phenetylalcohol **2**. Because of availability, we used deuterated ^{13}C-labeled methyl iodide although that is not a requirement since all the protons or deuterons are going to be removed during the subsequent steps. The next target step was the synthesis of phenylacetylene, which will provide the triple bond to which para-hydrogen can be added at a later stage. Starting from the secondary alcohol **2**, the exchange of the alcohol group for a bromo group was conducted via reaction with acetyl bromide (CAS 506-96-7). Subsequently, HBr was eliminated using potassium tert-butoxide (CAS 865-47-4) as a base to obtain a labeled styrene derivative **4**. Further addition of bromine to the double bond of the styrene unit resulted in its dibromo derivative (CAS 7726-95-6) **5**, which on double elimination of HBr in presence of sodium hydroxide (CAS 1310-73-2) gave ^{13}C-enriched phenylacetylene **6** as the desired intermediate. In the next step, phenylacetylene **6** was coupled with formaldehyde-d_2 (CAS 1664-98-8) to obtain the desired alcohol **7**, so completing the sidearm synthesis. We then further coupled ^{13}C-labeled alcohol **7** (Scheme 2) either with ^{13}C,^{2}H-labeled acetic acid (CAS 102212-93-1) or ^{13}C-labeled pyruvic (CAS 99124-30-8) acid to give the corresponding acetate **9a** or pyruvate ester **9b** in quantitative yields by using conventional DCC/DMAP peptide coupling agent.

3 | CONCLUSION

We have developed a synthetic route starting from benzaldehyde and ^{13}C-methyl iodide to produce phenylacetylene specifically ^{13}C-labeled in Position 2. This phenylacetylene is then further derivatized into an alcohol that is attachable to different metabolites such as acetate and pyruvate. The advantage of the presented sidearm is that it can be used in pulsed experiments independently of the magnetic field to enhance the signal

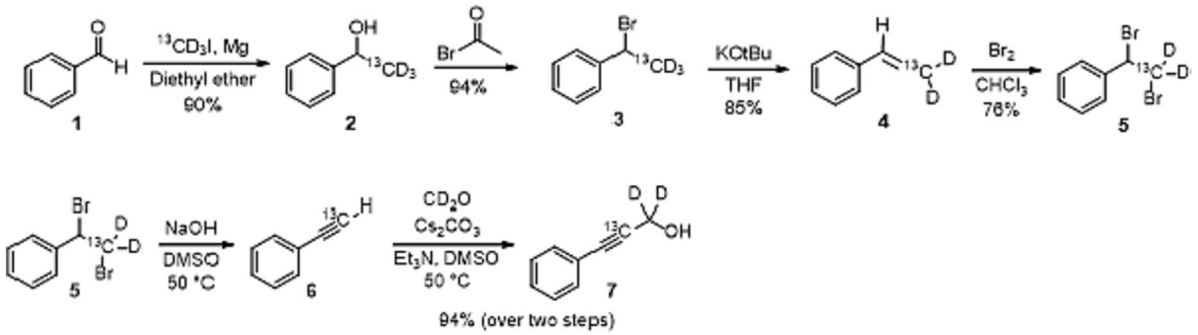

SCHEME 1 Synthesis of the sidearm.

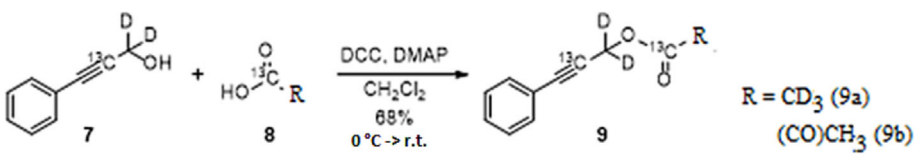

SCHEME 2 Synthesis of acetate and pyruvate derivatives for PHIP-SAH.

of ^{13}C-enriched metabolites, and we demonstrated it here at 21.5 mT fields. This can make the hyperpolarization procedure via PHIP-SAH more widely available since for most labs, no new NMR equipment needs to be available for the implementation of this approach. Therefore, we believe that the presented strategy provides easy access to real-time metabolic NMR.

4 | EXPERIMENTAL

4.1 | NMR studies at 21.5 mT

The field strength was chosen since it is close to the upmost limit of our available low field console (1 MHz, Kea2 from Magritek). This enabled us to obtain nutation curves for the pulse calibration in the shortest possible time. The samples for the PHIP experiments were prepared in the following way. By dissolving 9.41 mg of catalyst per 1 ml of acetone-d_6, 13 mM stock solutions of a Rhodium-based catalyst (rhodium[I] tetrafluoroborate, MW = 724.36, Sigma Aldrich 341134) were obtained. To obtain an acetone-d6 solution at 90 mM pyruvate precursor and 13 mM catalyst concentrations, 16.1 µl of pyruvate precursor (9b) (MW = 206.2, $\rho \sim 1.15$ mg/µl) were then dissolved per 1 ml of catalyst stock solution. Similarly, 4.7 µl of acetate precursor (9a) (MW = 181.2, $\rho \sim 1.15$ mg/µl) were dissolved per 1 ml of catalyst stock solution to obtain an acetone-d6 solution at 30 mM acetate precursor and 13 mM catalyst concentrations. Successively, 160 µl of precursor/catalyst/acetone-d_6 solutions was filled into 5 mm NMR tubes.

For the hyperpolarization experiments, the NMR tube was connected to a custom-built gas delivery system previously discussed[28] and preheated at 65°C for 2 min under 3 bar of nitrogen gas pressure. The NMR tube was then moved into the NMR magnet (21.5 mT), and the PHIP experiment was initiated. First, para-hydrogen enriched gas at 7 bar was bubbled via a capillary through the solution for 15 s, and then, the MINERVA sequence was applied for spin order transfer. Interestingly, the timings of the sequence are determined only by the J-couplings. Following the homology of the molecular structures, the J-couplings are similar for the pyruvate ($J_{HH} \sim 11.5$ Hz, $J_{CH1} < 0.5$ Hz, $J_{CH2} \sim 160$ Hz, $J_{CC} \sim 2.3$ Hz) and acetate ($J_{HH} \sim 11.8$ Hz, $J_{CH1} \sim< 1$ Hz, $J_{CH2} \sim 160$ Hz, $J_{CC} \sim 2.1$ Hz) substrates. The timings adopted for the MINERVA sequence were set according to $\tau_1 = \tau_3 = 1/(2J_{CH2})$, $\tau_2 = 1/(2J_{HH})$ $\tau_5 = 1/(2J_{CC})$, $\tau_4 = \tau_5$-τ_3. Explicitly, we used $\tau_1 = \tau_3 = 3.1$ ms, $\tau_2 = 43.5$ ms, $\tau_5 = 220.1$ ms, and $\tau_4 = 217$ ms for the pyruvate and acetate substrates.

The polarization levels were estimated following Mamone et al.,[33] by comparing the hyperpolarized signals to that of an equal volume of water recorded on the ^{13}C coil at a field scaled by the quotient of the proton-to-carbon gyromagnetic ratios $\gamma_{1H}/\gamma_{13C} \sim 4$. Briefly, the enhancement is calculated by considering the gamma ratio, the water-to-substrate concentration ratio, and the substrate-to-water integrated signal. The NMR signals are enhanced by about 10 million folds with respect to the corresponding thermal signals.

4.2 | Chemical synthesis

4.2.1 | Synthesis of **2**

To a stirred suspension of magnesium turnings (0.58 g, 24.5 mmol) in anhydrous diethyl ether (12 ml), dropwise iodomethane-^{13}C (1.41 ml, 22.6 mmol) in anhydrous ether (5 ml) was added. The resulting mixture was stirred at 25°C for 2 h. and a solution of **1** (1.91 ml, 18.8 mmol) in anhydrous diethyl ether (5 ml) was added dropwise at −5°C. The reaction mixture was gradually warmed to 25°C and stirred for 12 h. The reaction mixture was quenched with aq. NH_4Cl and extracted with ethyl acetate (3 × 15 ml). The combined organic layer was dried over Na_2SO_4 and was concentrated under reduced pressure to give **2** (2.1 g, 90% yield) as a colorless liquid.

TLC (Silica gel, 15% EtOAc in pet. ether), R_f (**1**) = 0.5, R_f (**2**) = 0.4, UV active.

^{1}H NMR ($CDCl_3$, 298 K, 300.13 MHz) δ = 7.22–7.36 (m, 5x ^{1}H), 4.85 (d, 1x ^{1}H, $^2J_{1H\text{-}13C}$: 1.75 Hz) ppm.

^{2}H NMR ($CDCl_3$, 298 K, 46.1 MHz) = 1.23 (dd, 3x ^{2}H, $^1J_{2H\text{-}13C}$: 19.36 and $^2J_{2H\text{-}13C}$: 0.81 Hz) ppm.

4.2.2 | Synthesis of **3**

Under N_2, atmosphere **2** (2.33 g, 18.5 mmol) was cooled to 0°C, and acetyl bromide (2.73 ml, 36.9 mmol) was added dropwise over 15 min. The reaction mixture was stirred at 27°C for 12 h. The excess of acetyl bromide was quenched by adding H_2O (15 ml) and extracted with diethyl ether (3 × 15 ml). The combined organic layer was dried over Na_2SO_4 and was concentrated under the reduced pressure to give **3** (3.29 g, 94% yield) as a yellowish liquid, which was used in the next step without further purification.

TLC (Silica gel, 10% EtOAc in Pet ether), R_f (**2**) = 0.3, R_f (**3**) = 0.7, UV active.

^{1}H NMR ($CDCl_3$, 298 K, 300.13 MHz) δ = 7.22–7.43 (m, 5x ^{1}H), 5.17 (d, 1x ^{1}H, $^2J_{1H\text{-}13C}$: 2.49 Hz) ppm.

^{2}H NMR ($CDCl_3$, 298 K, 46.1 MHz) = 1.43 (dd, 3x ^{2}H, $^1J_{2H\text{-}13C}$: 19.70 and $^2J_{2H\text{-}13C}$: 0.93 Hz) ppm.

4.2.3 | Synthesis of **4**

To a suspension of *t*-BuOK (4.88 g, 43.5 mmol) in anhydrous THF (12 ml), **3** (3.29 g, 17.4 mmol) was added dropwise in THF (3 ml). The resulting reaction mixture was stirred at 27°C for 12 h. The reaction mixture was then diluted with diethyl ether (20 ml), and the precipitate was removed by filtration. The filtrate obtained was carefully concentrated under the reduced pressure to give crude material, which was purified by flash column chromatography (silica) using gradient elution (100% pet ether) to give **4** (1.54 g, 85% yield) as a colorless liquid.

TLC (Silica gel, 100% Pet ether), R_f (**3**) = 0.4, R_f (**4**) = 0.6, UV active.

^{1}H NMR ($CDCl_3$, 298 K, 300.13 MHz) δ = 7.22–7.40 (m, 5x ^{1}H), 6.69 (s, 1x ^{1}H) ppm.

^{2}H NMR ($CDCl_3$, 298 K, 46.1 MHz, {^{1}H and ^{13}C-decoupling}) = 5.26 (s, 1x ^{2}H), 5.76 (s, 1x ^{2}H) ppm.

4.2.4 | Synthesis of **5**

Under a nitrogen atmosphere, bromine (2.64 ml, 16.6 mmol) was added dropwise to a cooled solution of **4** (1.54 g, 14.6 mmol) in $CHCl_3$ (15 ml). The resulting solution was stirred at 27°C for 30 min and was diluted with CH_2Cl_2 (10 ml). The organic layer was washed consecutively with a saturated solution of $NaHSO_3$, water, and brine. The combined organic layer was dried over Na_2SO_4 and was concentrated under the reduced pressure to give **5** (2.92 g, 76% yield) as a colorless liquid, which crystallizes upon cooling in the refrigerator.

TLC (Silica gel, 100% Pet ether), R_f (**4**) = 0.6, R_f (**5**) = 0.5, UV active.

^{1}H NMR ($CDCl_3$, 298 K, 300.13 MHz) δ = 7.29–7.37 (m, 5x ^{1}H), 5.10 (d, 1x ^{1}H, $^2J_{1H\text{-}13C}$: 4.71 Hz) ppm.

^{2}H NMR ($CDCl_3$, 298 K, 46.1 MHz) = 3.76 (d, 2x ^{1}H, $^1J_{1H\text{-}13C}$: 24.60 Hz) ppm.

4.2.5 | Synthesis of **6**

An aqueous solution of NaOH (1.82 g, 45.6 mmol, 2.64 ml of H_2O) was added to **5** (1 g, 3.80 mmol) in DMSO (4 ml). The resulting solution was heated at 50°C for 5 h. The reaction mixture was cooled to 27°C and diluted with water (15 ml). The aqueous solution was extracted with diethyl ether (3 × 15 ml). The combined organic layer was dried over Na_2SO_4 and was concentrated under the reduced pressure to give **6** as a colorless liquid, which was used in the next step without further purification.

TLC (Silica gel, 100% Pet ether), R_f (**5**) = 0.5, R_f (**6**) = 0.7, KMnO4 and UV active.

^{1}H NMR ($CDCl_3$, 298 K, 300.13 MHz) δ = 7.28–7.47 (m, 5x ^{1}H), 2.61 (d, 1x ^{1}H, $^1J_{1H\text{-}13C}$: 251.47 Hz) ppm.

4.2.6 | Synthesis of **7**

To a stirred solution of **6** (0.4 g, 3.88 mmol) in DMSO (8 ml) labeled formaldehyde-CD_2O (1 ml g, 6.20 mmol, 20% solution in D_2O), Et_3N (0.18 ml, 1.28 mmol), and Cs_2CO_3 (2.02 g, 6.21 mmol) were added. The resulting solution was heated to 60°C for 1 h. The reaction mixture was cooled to room temperature and quenched with water (20 ml). The aqueous layer was extracted with EtOAc (3 × 15 ml). The combined organic layer was washed with brine, dried over Na_2SO_4, and concentrated under reduced pressure. The crude product was purified by flash column chromatography (silica) using gradient elution (EtOAc: pet ether; 0:100 to 10:90) to give **7** (0.480 g, 94% yield over two steps) as a colorless liquid.

TLC (Silica gel, 10% EtOAc in pet. ether), R_f (**6**) = 0.8, R_f (**7**) = 0.3, $KMnO_4$ and UV active.

^{1}H NMR ($CDCl_3$, 298 K, 300.13 MHz) δ = 7.27–7.42 (m, 5x ^{1}H) ppm.

^{2}H NMR ($CDCl_3$, 298 K, 46.1 MHz, {^{1}H, ^{13}C-decoupling}) = 4.44 (s, 2x ^{2}H) ppm.

4.2.7 | Synthesis of **9a**

To a cold solution of **7** (0.25 g, 1.85 mmol), **8** (0.105 ml, 1.85 mmol), and DMAP (0.033 g, 0.278 mmol) in CH_2Cl_2 (10 ml) at 0°C, dropwise DCC (0.457 g, 2.22 mmol, dissolved in 5 ml of CH_2Cl_2) was added. The resulting solution was stirred to 27°C for 30 min and quenched by adding sat. solution of $KHSO_4$. The organic layer was separated, and the aqueous layer was extracted with CH_2Cl_2 (2 × 15 ml). The combined organic layers were dried over Na_2SO_4 and were concentrated under reduced pressure. The crude product was purified by flash column chromatography (silica) using gradient elution (CH_2Cl_2: pet ether; 0:100 to 70:30) to give **9** (0.23 g, 68% yield) as a colorless liquid.

TLC (Silica gel, 10% EtOAc in Pet. ether), R_f (**7**) = 0.3, R_f (**9**) = 0.6, UV active.

^{1}H NMR (600 MHz, $CDCl_3$) δ: 7.50–7.46 (m, 2x ^{1}H), 7.36–7.33 (m, 3x ^{1}H).

^{2}H NMR (92 MHz, $CDCl_3$) δ: 4.87 (s, 2x ^{2}H), 2.10 (s, 3x ^{2}H).

^{13}C-{^{1}H,^{2}H} NMR (151 MHz, $CDCl_3$) δ: 170.36 (d, $J = 2.8$ Hz), 131.91 (d, $J = 2.5$ Hz), 128.77 (d, $J = 1.0$ Hz), 128.30, 122.13 (d, $J = 13.0$ Hz), 86.50 (d, $J = 183.1$ Hz), 82.85 (d, $J = 2.8$ Hz), 52.33 (dd, $J = 80.2$, 2.3 Hz), 20.13 (d, $J = 58.8$ Hz).

LCMS: calculated for $C_9{}^{13}C_2H_5D_5O_2$: 181.1062, found 204.0988 (M + Na).

Synthesis of ***9b***: as previously described in Mamone et al.[33]

ACKNOWLEDGMENTS

This project has received funding from the H2020 European Research Council (ERC) under the European Union's Horizon 2020 research and innovation program (Grant Agreement No. 949180). S.G. acknowledges funding by the Max Planck Society. Open Access funding enabled and organized by Projekt DEAL.

CONFLICT OF INTEREST STATEMENT

S.G. is a co-founder of MagniKeen. The authors declare no competing financial interest.

PEER REVIEW

The peer review history for this article is available at https://www.webofscience.com/api/gateway/wos/peer-review/10.1002/mrc.5402.

ORCID

Stefan Glöggler https://orcid.org/0000-0003-3354-6141

REFERENCES

[1] R. W. Brown, Y. C. N. Cheng, E. M. Haake, M. R. Thompson, R. Venkatesan, *Magnetic resonance imaging: physical principles and sequence design*, Wiley, Hoboken, New Jersey **2014**.

[2] J. H. Ardenkjaer-Larsen, B. Fridlund, A. Gram, G. Hansson, L. Hansson, M. H. Lerche, R. Servin, M. Thanning, K. Golman, *Proc. Natl. Acad. Sci. U. S. A.* **2003**, *100*, 10158.

[3] K. Golman, R. In't Zandt, M. Thaning, *Proc. Natl. Acad. Sci. USA* **2006**, *103*, 11270.

[4] S. E. Day, M. I. Kettunen, F. A. Gallagher, D. E. Hu, M. Lerche, J. Wolber, K. Golman, J. H. Ardenkjaer-Larsen, K. M. Brindle, *Nat. Med.* **2007**, *13*, 1382.

[5] F. A. Gallagher, M. I. Kettunen, S. E. Day, D. E. Hu, J. H. Ardenkjaer-Larsen, R. in't Zandt, P. R. Jensen, M. Karlsson, K. Golman, M. H. Lerche, K. M. Brindle, *Nature* **2008**, *453*, 940.

[6] S. J. Nelson, J. Kurhanewicz, D. B. Vigneron, P. E. Z. Larson, A. L. Harzstark, M. Ferrone, M. van Criekinge, J. W. Chang, R. Bok, I. Park, G. Reed, L. Carvajal, E. J. Small, P. Munster, V. K. Weinberg, J. H. Ardenkjaer-Larsen, A. P. Chen, R. E. Hurd, L.-I. Odegardstuen, F. J. Robb, J. Tropp, J. A. Murray, *Sci. Transl. Med.* **2013**, *198*, 198ra108.

[7] J. Kurhanewicz, D. B. Vigneron, K. Brindle, E. Y. Chekmenev, A. Comment, C. H. Cunningham, R. J. DeBerardinis, G. G. Green, M. O. Leach, S. S. Rajan, R. R. Rizi, B. D. Ross, W. S. Warren, C. R. Malloy, *Neoplasia* **2011**, *13*, 81.

[8] C. R. Bowers, D. P. Weitekamp, *Phys. Rev. Lett.* **1986**, *57*, 2645.

[9] T. Trantzschel, J. Bernarding, M. Plaumann, D. Lego, T. Gutmann, T. Ratajczyk, S. Dillenberger, G. Buntkowsky, J. Bargon, U. Bommerich, *Phys. Chem. Chem. Phys.* **2012**, *14*, 5601.

[10] O. G. Salnikov, K. V. Kovtunov, I. V. Koptyug, *Sci. Rep.* **2015**, *5*, 13930.

[11] R. V. Shchepin, D. A. Barskiy, A. M. Coffey, I. V. Manzanera Esteve, E. Y. Chekmenev, *Angew. Chem. Int. Ed.* **2016**, *55*, 6071.

[12] K. V. Kovtunov, D. A. Barskiy, R. V. Shchepin, O. G. Salnikov, I. P. Prosvirin, A. V. Bukhtiyarov, L. M. Kovtunova, V. I. Bukhtiyarov, I. V. Koptyug, E. Y. Chekmenev, *Chem. A Eur. J.* **2016**, *22*, 16446.

[13] M. Haake, J. Natterer, J. Bargon, *J. Am. Chem. Soc.* **1996**, *118*, 8688.

[14] M. Goldman, H. Johannesson, O. Axelsson, M. Karlsson, *C. R. Chim.* **2006**, *9*, 357.

[15] P. Bhattacharya, E. Y. Chekmenev, W. H. Perman, K. C. Harris, A. P. Lin, V. A. Norton, C. T. Tan, B. D. Ross, D. P. Weitekamp, *J. Magn. Reson.* **2007**, *186*, 150.

[16] P. Bhattacharya, E. Y. Chekmenev, W. F. Reynolds, S. Wagner, N. Zacharias, H. R. Chan, R. Bünger, B. D. Ross, *NMR Biomed.* **2011**, *24*, 1023.

[17] A. B. Schmidt, S. Berner, W. Schimpf, C. Müller, T. Lickert, N. Schwader-lapp, S. Knecht, J. G. Skinner, A. Dost, P. Rovedo, J. Hennig, D. von Elverfeldt, J.-B. Hövener, *Nat. Commun.* **2017**, *8*, 14535.

[18] A. B. Schmidt, S. Berner, M. Braig, M. Zimmermann, J. Hennig, D. von Everfeldt, J.-B. Hövener, *PLoS ONE* **2018**, *13*, e0200141.

[19] A. B. Schmidt, M. Zimmermann, S. Berner, H. de Massin, C. A. Müller, V. Ivantaev, J. Hennig, D. V. Elverfeldt, J.-B. Hövener, *Commun. Chem.* **2022**, *5*, 21.

[20] S. Knecht, J. W. Blanchard, D. Barskiy, E. Cavallari, L. Dagys, E. van Dyke, M. Tsukanov, B. Bliemel, K. Münnemann, S. Aime, F. Reineri, M. H. Levitt, G. Buntkowsky, A. Pines, P. Blümler, D. Budker, J. Eills, *Proc. Natl. Acad. Sci. U. S. a.* **2021**, *118*, e2025383118.

[21] N. J. Stewart, H. Nakano, S. Sugai, M. Tomohiro, Y. Kase, Y. Uchio, T. Yamaguchi, Y. Matsuo, T. Naganuma, N. Takeda, I. Nishimura, H. Hirata, T. Hashimoto, S. Matsumoto, *Chem. Phys. Chem.* **2021**, *22*, 915.

[22] F. Reineri, T. Boi, S. Aime, *Nat. Commun.* **2015**, *6*, 5858.

[23] E. Cavallari, C. Carrera, M. Sorge, G. Bonne, A. Muchir, S. Aime, F. Reineri, *Sci. Rep.* **2018**, *8*, 8366.

[24] E. Cavallari, C. Carrera, S. Aime, F. Reineri, *J. Magn. Reson.* **2018**, *289*, 12.

[25] E. Cavallari, C. Carrera, S. Aime, F. Reineri, *Chem. Phys. Chem.* **2018**, *20*, 318.

[26] C. Carrera, E. Cavallari, G. Digilio, O. Bondar, S. Aime, F. Reineri, *Chem. Phys. Chem.* **2021**, *22*, 1042.

[27] J.-B. Hövener, A. N. Pravdivtsev, B. Kidd, C. R. Bowers, S. Glöggler, K. V. Kovtunov, M. Plaumann, R. Katz-Brull, K. Buckenmaier, A. Jerschow, F. Reineri, T. Theis, R. V. Shchepin, S. Wagner, P. Bhattacharya, N. M. Zacharias, E. Y. Chekmenev, *Angew. Chem. Int. Ed.* **2018**, *57*, 11140.

[28] S. Korchak, S. Yang, S. Mamone, S. Glöggler, *ChemistryOpen* **2018**, *7*, 344.

[29] S. Korchak, S. Mamone, S. Glöggler, *ChemistryOpen* **2018**, *7*, 672.

[30] S. Korchak, M. Emondts, S. Mamone, B. Blümich, S. Glöggler, *Phys. Chem. Chem. Phys.* **2019**, *23*, 22849.
[31] S. Korchak, A. P. Jagtap, S. Glöggler, *Chem. Sci.* **2021**, *12*, 314.
[32] Y. Ding, S. Korchak, S. Mamone, A. P. Jagtap, G. Stevanato, S. Sternkopf, D. Moll, H. Schroeder, S. Becker, A. Fischer, E. Gerhardt, T. F. Outeiro, F. Opazo, C. Griesinger, S. Glöggler, *Chemistry-Methods* **2022**, *2*, e202200023.
[33] S. Mamone, A. P. Jagtap, S. Korchak, Y. Ding, S. Sternkopf, S. Glöggler, *Angew. Chem. Int. Ed.* **2022**, *61*, e202206298. https://doi.org/10.1002/anie.202206298
[34] T. Hune, S. Mamone, H. Schroeder, A. P. Jagtap, S. Sternkopf, G. Stevanato, S. Korchak, C. Fokken, C. A. Müller, A. B. Schmidt, D. Becker, S. Glöggler, *Chem. Phys. Chem.* **2022**, *24*, e202200615.
[35] L. Dagys, A. P. Jagtap, S. Korchak, S. Mamone, P. Saul, M. H. Levitt, S. Glöggler, *Analyst* **2021**, *146*, 1772.
[36] L. Kaltschnee, A. P. Jagtap, J. McCormick, S. Wagner, L.-S. Bouchard, M. Utz, C. Griesinger, S. Glöggler, *Chem. A Eur. J.* **2019**, *25*, 11031.
[37] J. McCormick, S. Korchak, S. Mamone, Y. N. Ertas, Z. Liu, L. Verlinsky, S. Wagner, S. Glöggler, L.-S. Bouchard, *Angew. Chem. Int. Ed.* **2018**, *130*, 10852.
[38] A. B. Schmidt, A. Brahms, F. Ellermann, S. Knecht, S. Berner, J. Hennig, D. von Elverfeldt, R. Herges, J.-B. Hövener, A. N. Pravdivtsev, *Phys. Chem. Chem. Phys.* **2021**, *23*, 26645.
[39] R. W. Adams, J. A. Aguilar, K. D. Atkinson, M. J. Cowley, P. I. P. Elliott, S. B. Duckett, G. G. R. Green, I. G. Khazal, J. Lopez-Serrano, D. C. Williamson, *Science* **2009**, *323*, 1708.
[40] P. J. Rayner, M. J. Burns, A. M. Olaru, P. Norcott, M. Fekete, G. G. R. Green, L. A. R. Highton, R. E. Mewis, S. B. Duckett, *Proc. Natl. Acad. Sci. U. S. A.* **2017**, *114*, E3188.
[41] D. A. Barskiy, K. V. Kovtunov, I. V. Koptyug, P. He, K. A. Groome, Q. A. Best, F. Shi, B. M. Goodson, R. V. Shchepin, A. M. Coffey, K. W. Waddell, E. Y. Chekmenev, *J. Am. Chem. Soc.* **2014**, *136*, 3322.
[42] M. Suefke, S. Lehmkuhl, S. A. Liebisch, B. Blümich, S. Appelt, *Nat. Phys.* **2017**, *13*, 568.
[43] N. Eshuis, N. Hermkens, B. J. A. van Weerdenburg, M. C. Feiters, F. P. J. Rutjes, S. S. Wijmenga, M. Tessari, *J. Am. Chem. Soc.* **2014**, *136*, 2695.
[44] T. Theis, M. L. Truong, A. M. Coffey, R. V. Shchepin, K. W. Waddell, F. Shi, B. M. Goodson, W. S. Warren, E. Y. Chekmenev, *J. Am. Chem. Soc.* **2015**, *137*, 1404.
[45] P. Spannring, I. Reile, M. Emondts, P. P. M. Schleker, N. K. J. Hermkens, N. G. J. van der Zwaluw, B. J. A. van Weerdenburg, P. Tinnemans, M. Tessari, B. Blümich, F. P. J. T. Rutjes, M. C. Feiters, *Chem. A Eur. J.* **2016**, *22*, 9277.
[46] M. L. Truong, F. Shi, P. He, B. Yuan, K. N. Plunkett, A. M. Coffey, R. V. Shchepin, D. A. Barskiy, K. V. Kovtunov, I. V. Koptyug, K. W. Waddell, B. M. Goodson, E. Y. Chekmenev, *J. Phys. Chem. B* **2014**, *118*, 13882.
[47] J. F. P. Colell, M. Emondts, A. W. J. Logan, K. Shen, J. Bae, R. V. Shchepin, G. X. Ortiz Jr., P. Spannring, Q. Wange, S. J. Malcolmson, E. Y. Chekmenev, M. C. Feiters, F. P. J. T. Rutjes, B. Blümich, T. Theis, W. S. Warren, *J. Am. Chem. Soc.* **2017**, *139*, 7761.
[48] W. Iali, S. S. Roy, B. J. Tickner, F. Ahwal, A. J. Kennerley, S. B. Duckett, *Angew. Chem. Int. Ed.* **2019**, *58*, 10271.
[49] P. TomHon, M. Abdulmojeed, I. Adelabu, S. Nantogma, M. S. H. Kabir, S. Lehmkuhl, E. Y. Chekmenev, T. Theis, *J. Am. Chem. Soc.* **2022**, *144*, 282.
[50] A. B. Schmidt, H. de Maissin, I. Adelabu, S. Nantogma, J. Ettedgui, P. TomHon, B. M. Goodson, T. Theis, E. Y. Chekmenev, *ACS Sensors* **2022**, *7*, 3430.
[51] T. L. K. Hune, S. Mamone, A. B. Schmidt, I. Mahú, N. D'apolito, D. Wiedermann, J. Brüning, S. Glöggler, *Appl. Magn. Reson.* **2023**, 1. https://doi.org/10.1007/s00723-023-01578-z

How to cite this article: A. P. Jagtap, S. Mamone, S. Glöggler, *Magn Reson Chem* **2023**, *61*(12), 674. https://doi.org/10.1002/mrc.5402